



Hydroisomerization of n-Heptane in a Fixed-Bed Reactor Using a Synthesized Bimetallic Type-HY Zeolite Catalyst

Younus H. Khalaf ^{*}, Bashir Y. Sherhan, Zaidoon M. Shakor

Chemical Engineering Dept., University of Technology-Iraq, Alsina'a street, 10066 Baghdad, Iraq.

*Corresponding author Email: che.19.22@grad.uotechnology.edu.iq

HIGHLIGHTS

- The synthesis of NaY-zeolite by the hydrothermal method.
- Modification of NaY to form NH₄Y, HY, and Metal-Loaded-HY-Zeolites by incipient wetness impregnation method
- The preparation of the bimetallic catalyst depends on the two metals Zr and Pt.
- Performing the hydroisomerization of n-heptane and proving the novel catalyst (1wt% Pt with 1wt% Zr)/ HY-Zeolite is an active and selective catalyst.
- The amount of the costly Pt metal in the catalyst depends on the cheap Zr Metal was decreased.

ABSTRACT

The synthesis of NaY-zeolite was performed hydrothermally. The preparation of the bifunctional catalysts was achieved by loading NH₄Y-zeolite with a cheap Zr metal, as a second loading metal, with tiny amounts of Pt to compose a Pt-Zr/Y-zeolite catalyst. Different characterization methods (i.e., XRD, SEM, EDX, BET, and AFM) were used to investigate the catalyst properties. The catalytic performance was studied by performing the hydroisomerization of n-heptane in a gas phase at a temperature of 275°C and atmospheric pressure in a fixed-bed reactor. The GC-FID results of the products confirmed the positive role of Zr in enhancing the catalytic features, as reflected by the increase in the isomerized products and the decrease in the unwanted by-products. Incorporating 1.0wt%Zr with 1.0wt% of Pt significantly improved the activity and selectivity and increased the yield of branched alkanes. This was achieved because the addition of zirconium provided an extraordinary Lewis acidity to the zeolite-framework structure and simultaneously took advantage of the electronic and catalytic properties of Zr and Pt metals to enhance its novel catalytic features. This reduced the amount of Pt metal and halved the cost of the catalyst. In addition, the bimetallic catalyst (HY-zeolite loaded with 1wt%Pt & 1wt%Zr) achieved values of 74.2, 78.8, and 58.5mol% for conversion, selectivity, and yield, respectively. The conversion was improved to a level close to 2wt% Pt/HY-zeolite catalyst, while selectivity was not significantly decreased from that of 2wt% Zr/HY-zeolite catalyst, reaching a yield level of isomers close to that of 2wt% Pt/HY-zeolite catalysts.

ARTICLE INFO

Handling editor: Mustafa H. Al-Furaiji

Keywords:

Bimetallic; Isomerization; Octane, Platinum Synthesis; Zirconium

1. Introduction

One of the most important objectives of every petroleum refining industry is to use the hydroisomerization process, which converts crude oil into various derivatives, particularly high octane fuel. From an economic viewpoint, light alkanes (C₄–C₇) isomerization has been a profitable option for the petroleum refining industry due to the continuously growing demand for isomerized products over the past decades. This resulted in achievements and significant strides in isomerization technologies, improving the quantity and quality of products [1-3]. The isomerization process is generally described as due to the existence of dual-functional catalysts composed of solid acid catalysts loaded with a noble metal currently applied in industrial processes. These bifunctional catalysts are composed of two components with two functions; the first component, e.g., the HY-zeolite, is utilized to provide the acidic function, and the second component, e.g., the Pt metal, is employed to provide the metallic function, being responsible for the dehydrogenation–hydrogenation effect [4-5]. When the bifunctional catalyst's two components (i.e., metallic and acidic) are used together, high levels of catalytic activity, selectivity, and stability are achieved [4,6]. According to the isomerization mechanism, the dehydrogenation of the feed alkanes is performed on the metallic site. Then the formation of carbonium ions from olefins and rearrangements occurs on the acidic sites. Afterward, hydrogenation of the isomerized olefins takes place on the metallic site to give the isomerized alkanes [4-5,7]. Many solid acid catalysts, such as aluminum chloride, chloride alumina, silica gel, and sulfated zirconia, have been used in the isomerization process. However,

due to their superior properties, the zeolite-based catalysts were more suitable and practical than the other solid catalysts. Noble metals supported on zeolites and used in the isomerization process not only activate C-H, H-H, and C-C bonds but also protect the catalyst surface from deactivation. They achieve the latter function by preventing coke deposition, with the help of hydrogen, to keep the catalyst surface clean of heavy hydrocarbons [8-10].

Commonly, noble metals, such as Pd and Pt, are loaded on supporting catalysts, such as zeolite, as single atoms in the pores and cavities. These are prepared by post-synthetic cation exchange procedures, where the corresponding metal salt is exchanged in a medium or large pore zeolite type, preferentially Y, ZSM-5, or Beta [11-13]. The crystalline nature of zeolites could mostly preclude the metal agglomeration under reaction conditions or during catalyst regeneration, allowing the increase in the catalyst activity and the catalyst lifetime. When metallic heteroatoms other than aluminum are introduced in the tetrahedral crystalline frameworks of zeolites, it was found that they create physicochemical properties different from those of the zeolite-based catalysts and greatly enhance their catalytic properties. This opens new opportunities for catalytic implementation in novel chemical processes [14-17]. These different heteroatoms (i.e., Zr, Ti, Sn, Nb, and Ta) are tetrahedrally substituted metals into zeolite frameworks. In addition, incorporating these metals in tetrahedral coordination provides an extraordinary Lewis acidity to the zeolite-based catalyst; in particular, the Sn- and Zr- containing zeolites have received significant attention in the last years, allowing their implementation as very active and selective catalysts [18-27].

Many researchers are still exerting remarkable efforts to find other metals that can contribute to decreasing the amount of the costly Pt metal, especially in the bimetallic catalysts' field. Among those, Wang and Zhang studied the catalysts MCM-48, Zr-MCM-48, and Ni/H-Zr-MCM-48 by n-heptane isomerization as a probe reaction]. Compared with MCM-48, Zr-MCM-48, and H-Zr-MCM-18, the bimetallic catalyst Ni/H-Zr-MCM-48 exhibited significantly higher selectivity for forming isoparaffin, with lower coke deposition and excellent catalyst stability [28]. Karakoulia examined the hydroisomerization reaction of n-octane on a series of monometallic and bimetallic Pt (0.2 wt.%) and/or Ni (10 wt.%) catalysts supported on β -zeolite. He found that the addition of Pt in the bimetallic Ni-Pt catalyst not only activates but also improves the isomerization selectivity, favoring the production of di-branched rather than mono-branched isomers [29]. Furthermore, Kitaev and Burkina examined a bimetallic catalyst made of 0.2-0.8 wt% Zr- and 0.5wt% Pt loaded on the dealuminated Zeolite (USY). The acid properties and catalytic activity were studied in n-hexane conversion. They found that zirconyl nitrate contributes to forming strong acid sites, improving cracking activity in n-hexane conversion [30]. Yang investigated a novel bimetallic isomerization of Pt-NiP/H β catalyst by incorporating a small quantity of Pt into the NiP compound on H β zeolite. He proved that this bimetallic catalyst demonstrated a distinguished catalytic activity compared to Pt/H β and NiP/H β catalysts for hydroisomerization of normal hexane [31].

By reviewing the literature, a lack was noticed in studies that compare the behavior and physical properties of the type Y catalyst in its acidic form, which is loaded with only one metal (i.e., Monometallic: either Pt or Zr), with the behavior of the two-metal loaded catalyst (i.e., Bimetallic: Pt and Zr) in hydroisomerization reactions. In this work, a cheap Zr metal was selected to enhance the catalytic properties of the HY-Zeolite catalyst. The performance of the 1%Pt-1%Zr/HY catalyst was accurately compared with that of both 2%Pt/HY and 2%Zr/HY catalysts. Therefore, the catalysts were synthesized and modified for the hydroisomerization of n-heptane with an octane number of zero. The effects of modification on catalytic activity and catalytic selectivity were experimentally investigated. The aim was to prepare an active catalyst with exceptional Lewis acidity by loading zirconium metal. This catalyst should also be sufficient to compensate for the reduction in the amount of rare and expensive metals, such as platinum, within the HY zeolite catalyst and suitable for hydrogenation and dehydrogenation reactions.

2. Experimental

2.1 Materials

The following chemical reagents were purchased from commercial providers. sodium aluminate (NaAlO_2 : 50.9 wt.% Al_2O_3 +31.2 wt.% Na_2O + 17.9 wt.% H_2O) was provided by Sigma-Aldrich. Ludox AS-40 colloidal silica (40 wt%) suspension in H_2O was provided by Sigma-Aldrich, USA. Sodium hydroxide, pellets a. r. NaOH (99%) was provided by CHEM-LAB, Belgium. De-ionized water was provided by an Iraqi manufacturer. Ammonium chloride (NH_4Cl) was provided by SDFCL-SD FINE-CHEM, India. Hexo-chloroplatinic acid H_2PtCl_6 was provided by Sigma-Aldrich. Zirconyl nitrate: $\text{ZrO}(\text{NO}_3)_2 \cdot \text{H}_2\text{O}$ (99.5%), provided by Oxford Lab Chem-India. Hydrogen (99.9%) was provided by Petroleum R&D Center-Baghdad, Iraq. n-heptane (99 %) was provided by CHEM-LAB, Belgium.

2.2 Catalyst Synthesis

This research's experimental work included synthesizing NaY, NH_4Y , HY, and metal/HY-zeolite forms.

2.2.1 Nay-Zeolite Synthesis Process

The hydrothermal process was applied using laboratory-grade chemicals (Ludox, sodium aluminate, sodium hydroxide, and de-ionized water). The NaY-zeolite was synthesized by the hydrothermal method depending on a chemical recipe of the FAU structure with the chemical formula: $\text{Na}_{56} [\text{Al}_{56} \text{Si}_{136} \text{O}_{384}] : 250 \text{H}_2\text{O}$. Chemicals used in this process are Ludox (source of silica), sodium aluminate, de-ionized water, and sodium hydroxide. The preparation procedure is available in the Verified Syntheses of Zeolitic Materials Handbook [32-33]. The manufacturing procedure diagram is shown in Figure 1 .

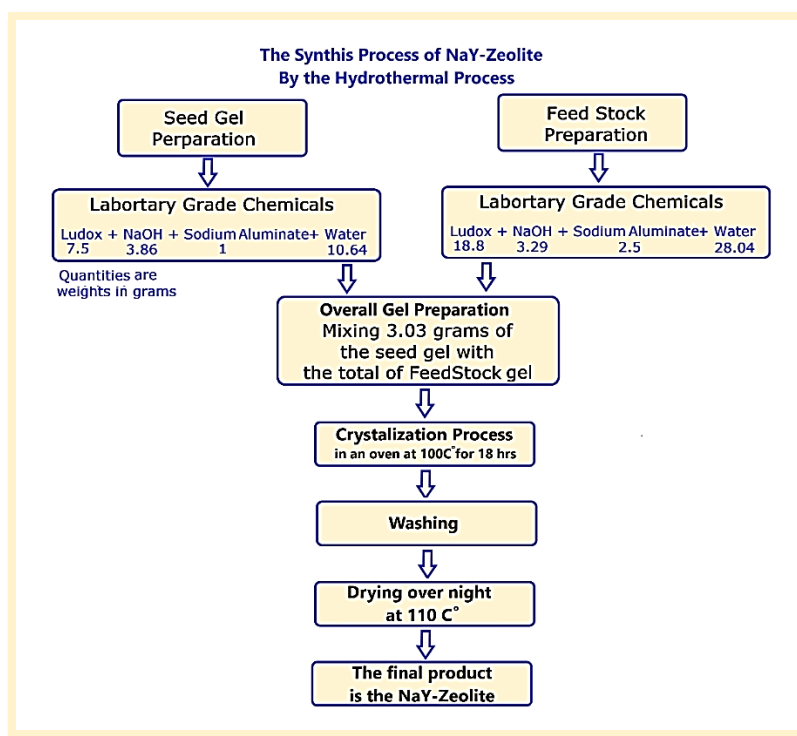


Figure 1: Steps of the hydrothermal synthesis process of NaY zeolite

The preparation method requires the synthesis of two gels, namely those of seed and feedstock, which are made according to the following percentages: Batch composition: Feedstock gel (95% Al): 4.30 Na₂O: Al₂O₃: 10 SiO₂: 180 H₂O, seed gel (5% Al): 10.67 Na₂O: Al₂O₃: 10 SiO₂: 180 H₂O, overall gel 4.62 Na₂O: Al₂O₃: 10 SiO₂: 180 H₂O.

2.2.1.1 Seed gel preparation:

Seed gel was prepared firstly by blending the exact weight of all materials; 1 g of Sodium aluminate (NaAl₂O₃), 10.64 g of de-ionized water (H₂O), and 3.86 g of Sodium hydroxide (NaOH). These materials were mixed in a polypropylene plastic bottle until the solids were fully dissolved in the solution. Then, 7.5 g of Ludox “colloidal SiO₂” As-40 wt% was carefully added to the bottle using a pipette, and the mixture was mixed for at least 10 min using a magnetic stirrer. Finally, the slurry was left to age at room temperature for nearly one day.

2.2.1.2 Feedstock gel preparation:

On the second day, feedstock gel was prepared by blending the exact weight of the same chemical materials (i.e., 2.5 g of NaAl₂O₃, 3.29 g of NaOH, and 28.04 g of de-ionized water) in another plastic bottle. After that, 18.8 g of colloidal silica (Ludox) was added. All the chemicals were mixed strongly for 10 minutes until white aluminosilicate gel was clearly formed.

2.2.1.3 Overall gel preparation:

The final gel was produced by slowly mixing the required amount of the seeding gel with the feedstock gel to produce the overall gel, which was vigorously blended for twenty minutes. The overall gel was subsequently heated in an oven at 100 °C for 18 h to secure adequate crystallization time. The sample was later taken out of the oven, centrifuged for about 15 minutes, and then washed with distilled water until the pH fell to less than 9 or, more preferably, approximately 7. Finally, the wet powder product of NaY zeolite was dried overnight at 110 °C [32-33].

2.2.2 Ion-exchange process and HY-zeolite production

The produced zeolite contains sodium ions. This cation should be replaced with a proton (H⁺) to make a zeolite in its acidic form. Thus, the removal of sodium was achieved by utilizing the ion-exchange method, using the NH₄Cl; a weight of 1 gm of NaY-zeolite was placed in a 100 ml ammonium chloride aqueous solution (0.5 M). The mixture was heated at 80 °C under reflux conditions with constant stirring for one hour. Three times multi-stage ion exchange procedure was required, using the above conditions, to remove the sodium ion to less than 0.5 wt%. It was found that the exchange level increased with increasing the number of exchanged steps. Afterward, the exchanged zeolite (NH₄Y-form) was filtered off, washed with one liter of distilled water, centrifuged for about 10 min, and then dried at 110 °C overnight. To prepare an anhydrous crystalline HY-zeolite, the NH₄⁺ cations were decomposed to give ammonia and protons. This was performed in subsequent steps by a calcination process (i.e., heat treatment under airflow) at 450 °C under 10 °C/min for 3 hrs in a programmable furnace. The prepared material was then introduced into the metal loading process, as demonstrated in Figure 2.

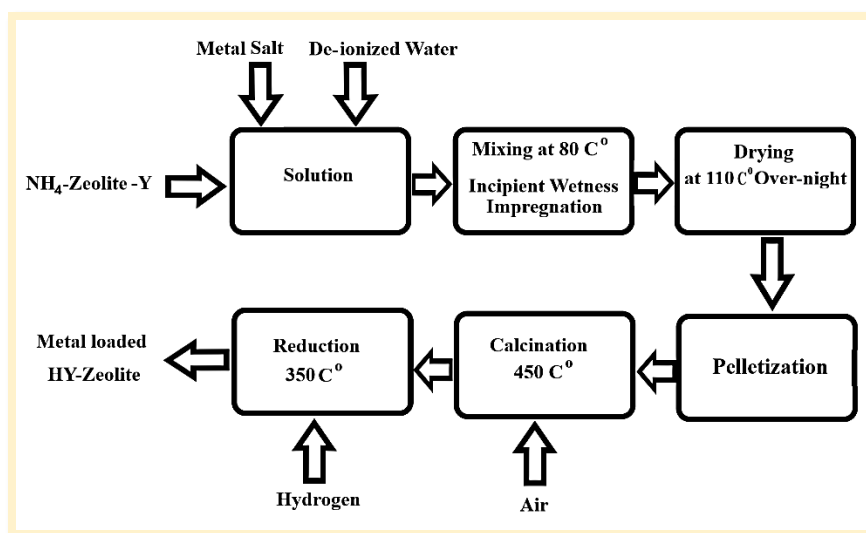


Figure 2: Flowchart of the preparation of the NH₄Y-zeolite catalyst

2.2.3 Composing of the bifunctional catalyst

The modification step of the synthesis process to obtain the bifunctional catalyst was performed by loading the NH₄-zeolite with a metal (i.e., Pt and Zr) by following the incipient wetness impregnation method (IWI). The method is performed as follows: 1 gm of the ammonium form of zeolite catalyst was placed in 100 ml of distilled water. The Zr and/or Pt salt was dissolved in water. The amount was calculated to result in the desired percentage of the loaded metal. H₂PtCl₆ Hexo-ChloroPlatinic acid was used as a source of Pt and Zirconyl nitrate [ZrO(NO₃)₂.H₂O] as a source of Zr. The mixture was heated at 80 °C with constant stirring for two hours, as given in Figure 2. Afterward, the impregnated NH₄Y-zeolite was filtered off, washed with one liter of distilled water, and centrifuged for 10 min under 3500 rpm. The drying process was subsequently applied overnight at 110 °C to obtain the product of Pt-Zr/HY-zeolite catalyst. Next, catalysts were prepared by loading 2wt% from each metal type for making the bifunctional catalysts, which were also prepared using the wet incipient impregnation method. The reduction process was conducted *in situ* in the presence of hydrogen gas at 350 °C for 2 hrs inside the fixed-bed reactor [16,32,34]. Three catalysts were prepared with different ratios of metals are shown in Table 1.

2.2.4 Catalysts pelletizing v

After completing the synthesis process of bifunctional zeolite catalysts, which form fine powders, they cannot be used in the reactor directly because it causes the back pressure problem. Therefore, these catalysts should be shaped into pellets of the size of 125-450 micrometers using a hydraulic pressing machine. The powders were pressed under about 15 tones/m². A value of 15 tons/m² represents the pressure applied by the pressing machine and used to shape the powder sample over a given area. Approximately 4 grams of each prepared zeolite catalyst was pressed and shaped into discs of 23 mm in diameter. Afterward, these large discs were crushed with a pestle and mortar to shape the catalysts in the form of small pellets. Subsequently, they were cautiously sieved in a mesh sieve to select the particles with sizes between 125-450 μm to obtain uniform catalyst particles.

2.3 Characterization of the Synthesized Catalysts

The XRD analysis was performed using the SHIMADZU Lab X XRD-6000 diffractometer, Japan; the scan rate was 0.2 Degrees. Cu (1,5406 Å), with a voltage of 40.0 kV and a current of 30.0 mA. SEM & EDX apparatus (Inspect S50) was used to obtain the Si/Al bulk ratio, elemental composition (i.e., sodium content), crystal morphology of catalyst particles, and direct measurement of the crystal size. In addition, the BET-surface area and pore volume of the synthesized zeolite was determined based on Brunauer Emmett and Teller's (BET) method using an analyzer (Q Surf 1600, USA). Atomic Force Microscopy (AFM) is one of the new groups of scanning probe microscopies. In this system, a mechanical probe consisting of a tip with atomic dimensions moves over the sample surface. The derived signals can be converted into images with a lateral resolution of 20 nm in the principal surface plane of the sample. In addition, it is sensitive to particles 1 nm in size in the vertical dimension. The analysis was performed by a second-generation tabletop Atomic Force Microscope- TT-2AFM.

Table 1: The prepared bifunctional catalysts

No.	Code	Catalyst Composition
1	Cat-1	HY-zeolite + 2 wt % Pt
2	Cat-2	HY-zeolite + 2 wt % Zr
3	Cat-3	HY-zeolite + 1 wt% Pt + 1 wt% Zr

2.4 Catalytic Experiments

The catalytic performance measurements of the synthesized Y-catalysts were conducted for the hydroisomerization of n-heptane in a continuous-flow fixed-bed stainless steel reactor (8 mm inner diameter, 600 mm length), which is surrounded by a vertical furnace to be heated with a temperature controller. A thermocouple was used to measure the temperature inside the reactor, which is fixed inside the reactor under atmospheric pressure conditions. For each hydroisomerization experiment, the reactor was packed with the desired amount of catalyst (about 4 g) as pellets with a size range of 125–450 μm to avoid the back-pressure effect. Hence, a pressure gauge was utilized to check the pressure drop inside the system. Basically, the loaded Y-catalysts should be sandwiched between two layers of glass beads. Several valves were employed further to control the gas flow through the piping system. Three connected bubblers were half-filled with liquid n-heptane to introduce the feed to the reactor. This glass bubbler Figure 3. was bought from the glassware manufacturing plant in United Kingdom. The bubbler was put in a cold bath surrounded by ice cubes at about 0 °C to make the contact time constant during the reaction. In fact, the average value of mol% of n-heptane in the feed had to be kept constant as the temperature of the cold bath was fixed, and the flow of hydrogen was also constant. The gas stream was passed through a gas purifier before carrying away the nC₇ molecules from the bubblers into the fixed catalyst bed inside the reactor.

A flow meter and valve were also utilized to control the flow of hydrogen that passes through the bubbler and exits saturated with the n-heptane to enter the reactor. Stainless steel tubes with 8 mm I.D. were used to connect the bubblers with the reactor. All tubes were held constant at approximately 150 °C using an electrical heater and covered with an insulation layer, thereby avoiding the condensation of n-heptane vapor feed. The hydroisomerization reaction was performed inside the reactor, and the products from the reaction were collected and then analyzed by GC-FID to identify the different components. The schematic diagram of the hydroisomerization experimental system is shown in Figure 4. As mentioned earlier, before the reaction, the catalyst was reduced under H₂ flow at 350 °C for 2 h. Afterward, the reactor was left to cool, and the temperature was adjusted to the desired values (i.e., 275 °C), then the feedstock of n-heptane was continuously fed into the reactor. Finally, the product was condensed at 0 °C and samples were collected after 15 min on stream. Then, they were analyzed using a GC-FID detector.

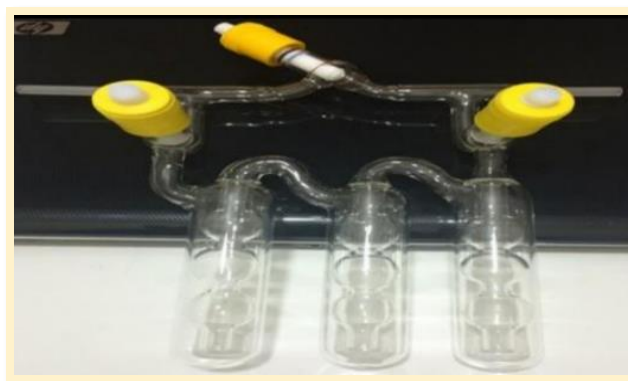


Figure 3: The three connected bubblers

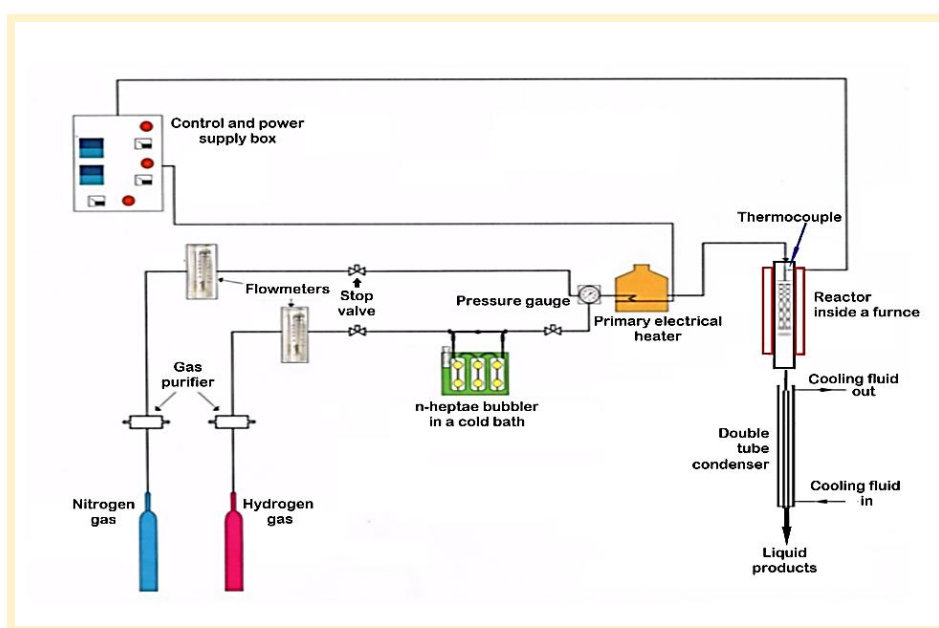


Figure 4: The schematic diagram of the hydroisomerization unit

3. Results and Discussion

3.1 XRD-Pattern of the Synthesized NaY-Zeolite

To prove the successful synthesis of NaY-zeolite by the hydrothermal method, a crystalline structure of the synthesized zeolite-Y was obtained, as shown in XRD-test in Figure 5. The pattern of this sample indicates that the structure of the synthesized zeolite sample has approximately the same pattern and equal major peaks in comparison with the XRD pattern of the standard zeolite Faujasite the referenced by International Zeolite Association (IZA), which is shown in Fugre 6 [32,33]. When the major peaks in the synthesized sample exist in identical positions with the major peaks of the standard Faujasite pattern, this confirms that the sample is a Faujasite type. The X-Ray Diffraction of any sample must occur at the same peak position (2θ°) for the standard sample according to Bragg's law [35]. This is because the XRD pattern is typically utilized as a fingerprint for each crystalline solid, such as zeolite-Y. This means that the NaY-zeolite synthesis process was passed successfully [36].

On the other hand, it can be seen in

F that the full width of the peak at half maximum (FWHM) becomes broader as the average size “dimensions” of the crystal decreases, according to the Scherrer’s law [35]. In addition, the Y-structure in the figure shows an increase in the size of the crystals according to the above the law. It can also be predicted that the degree of crystallization is high with the decrease of amorphous materials. As a rule, highly crystalline zeolite samples must have quite a flat baseline with relatively high intensities of peaks.

The percentage of crystallinity for the synthesized NaY-zeolite sample was calculated from the sum of intensities of the main peaks given from the XRD machine, according to equation (1), by dividing the sum of the main peak intensities of the synthesized NaY-zeolite by the sum of the main peak intensities of the reference Y-zeolite [32]. Table 2 shows the crystallinity of the synthesized sample with almost high crystallinity. It confirms the purity of framework structures of the synthesized sample.

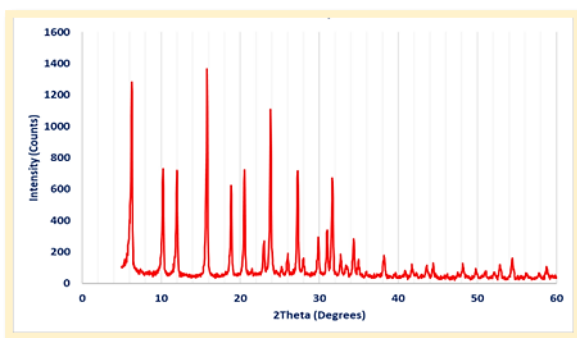


Figure 5: FXRD-test of the synthesized NaY-zeolite sample

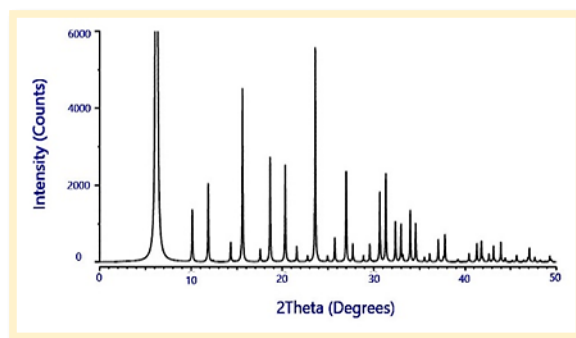


Figure 6: XRD-test of the standard NaY-zeolite [32]

$$\text{Degree of Crystallinity (\% DOC)} = \frac{\text{Sum of main peak intensities of the synthesized Y-zeolite}}{\text{Sum of main peak intensities of the Reference Y-zeolite}} \tag{1}$$

Where % DOC is a percentage degree of crystallinity using the standard Faujasite as a reference.

Table 2: XRD-Analysis data of the synthesized NaY-zeolite

The standard Faujasite 2θ °	Intensity (I)	The synthesized 2θ °	Sample Intensity(I)
6.2330	100	6.40730	95
15.640	53	15.8457	100
20.360	38	20.5759	58
23.635	59	23.8775	82
27.042	39	27.2929	54
30.730	22	29.8931	18
31.378	49	31.6715	52
32.432	16	32.7318	10
34.053	15	34.3699	20
Sum	391		489
%DOC	100%		125.07%

3.2 SEM and EDX Analyses

The synthesized Na-Y zeolite sample was investigated using SEM with different magnifications. From SEM images, it is clear that the zeolite powder is uniformly composed of fine particles, while there is no clear agglomeration in a large block. This observation agrees with the X-ray diffraction analysis results, and the sample was noticeably identified as having the desired zeolite Na-Y morphology. As shown in Figure 7, the zeolite particle clusters consist of semi-spherical and cubic crystals ranging between 2-5 μm in length.

Some crystals showed growth on all sides, which is generally rationalized by a high nuclei concentration. Y-crystal development was evident at the scale of 5 μm and occurred during a crystallization time of 18 hr, which is considered the optimum time for maximum crystallization [32]. It is clear in the above figures that crystals have sharp edges, large sizes, and a uniform shape, which confirms that the crystallization process was completed.

On the other hand, the contents of silicon, aluminum, sodium, and the loaded metals on the external surface of the NaY-zeolite crystal were identified using dispersive energy X-ray (EDX) attachment of the SEM analysis. EDX analysis of the NaY-zeolite form stated the percentages of the elements that compose the zeolite. The bulk ratio of (Si/Al) is 2.41, which is mostly in good agreement with the standard ratio of Faujasite type Y-zeolite (i.e., 1.5-3) [32-33]. In addition, the concentration of Na within the framework of fresh NaY-zeolite is 8.3wt%, as shown in Figure 8 -a. In fact, the resulting zeolite contains an unwanted sodium ion. This cation must be replaced by an H^+ proton to bring the zeolite into the acidic form. Therefore, as previously mentioned, the sodium ion is removed firstly by multi-stage ion-exchange methods using NH_4Cl salt. As a result, the sodium ion concentration decreased from 8.3 wt% to 0.25 wt%, as shown in Figure 8-a,b, which is in the acceptable range and shows that the ion-exchange processes with ammonium chloride have been carried out successfully.

Metals were loaded onto the surface of the synthetic $\text{NH}_4\text{-Y}$ -zeolite catalysts using the wetness incipient impregnation method. First, loading processes were done with two concentrations of 2wt% of each metal to prepare the two catalysts (2 wt% Zr/HY for Cat-1 and 2 wt% Pt/HY for Cat-2). Then the bimetallic catalyst Cat-3 (1.0wt% Pt with 1wt%Zr on HY) was prepared by loading the $\text{NH}_4\text{-Y}$ -zeolite form with the two metals Pt & Zr according to the precisely calculated quantities. Its EDX test showed the metal loading process was successful, as shown in Figure 8-c.

3.3 BET Results

The surface area of an HY-zeolite sample synthesized during 18 hours of crystallization time was analyzed using the Brunauer Emmett and Teller (BET) method. The results confirmed that the surface area of the synthesized sample is 483.4 m^2/g . Furthermore, the result of BET analysis showed that the surface area of the synthesized HY-zeolite agrees with the standard BET values of HY-zeolite [32,37-38].

3.4 AFM Analysis

The morphology and the particle diameter of the synthesized HY-zeolite were investigated using Atomic Force Microscope (AFM) with three-dimensional surface profiles. The 3D surface image shown in Figure 9-Right confirms that the zeolite particles are crystalline in shape and uniformly agglomerated. AFM observation identified that the diameters of the prepared zeolite particles were in the range of 34-66 nm, as shown in Figure 9-Left, demonstrating the particle size distribution of HY-zeolite. The results confirm that the average diameter of zeolite particles is 43.88 nm. Table 3 corroborates that the highest volume percentage was 12.89 % for the particle size distribution of 36 nm and the lowest volume percentage was 0.15 % for the diameter of 66 nm.

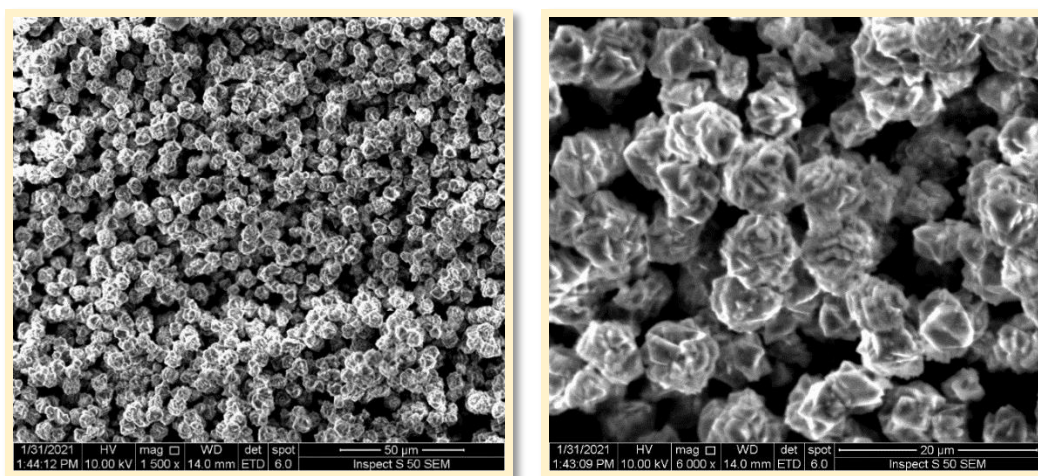


Figure 7: SEM-images of NaY-zeolite with magnification of, (Left) 1500X, (Right) 6000X

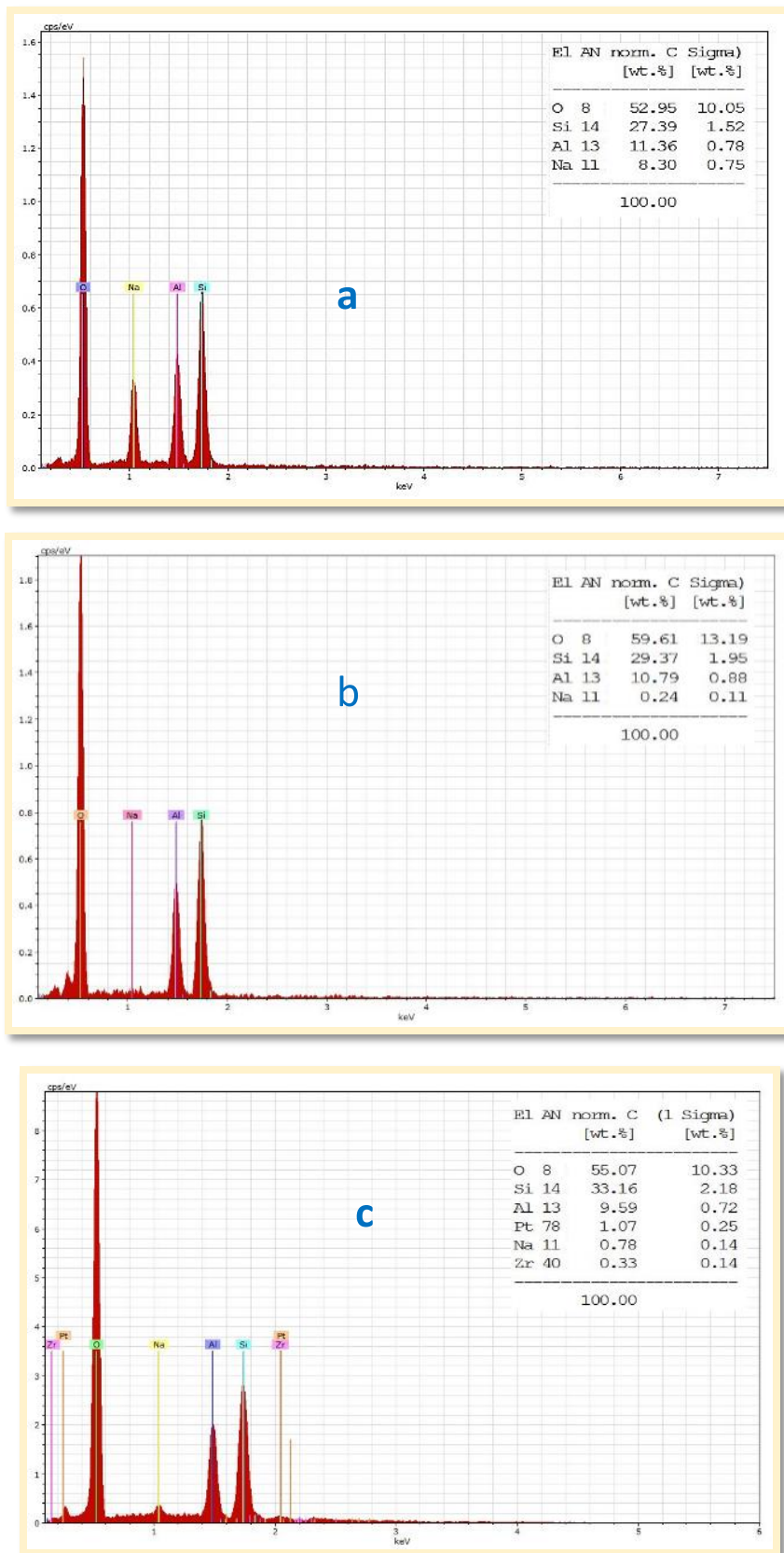


Figure 8: EDX tests of (a)- NaY-sample, (b)-NH₄-Y sample, (c)- HY-loaded with (1.0wt%Zr and 1.0wt% Pt)

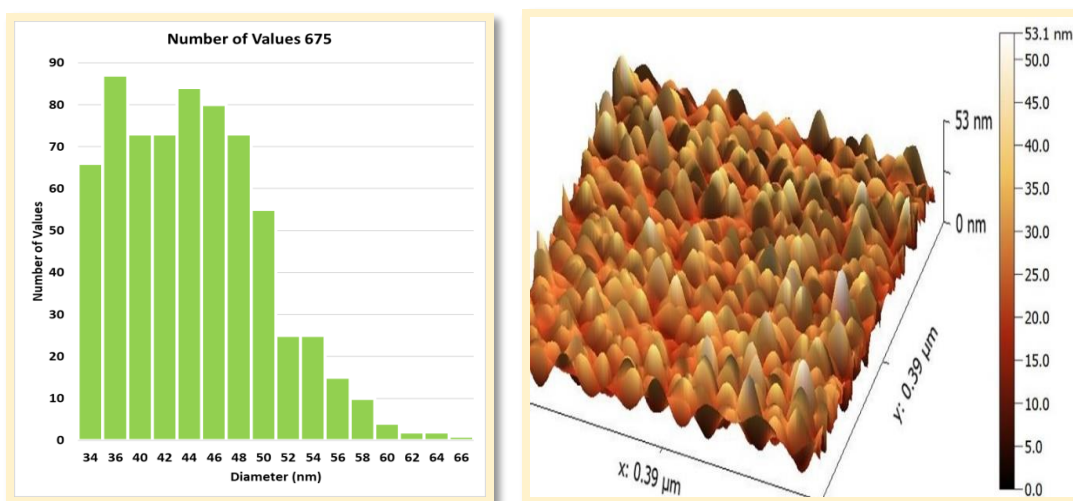


Figure 9: (Left) Particle size distribution of HY- zeolite and (Right) AFM of HY-zeolite surface

Table 3: Particles size distribution of HY-zeolite with an average diameter of 43.88 nm

Diameter	No. Of	Volume	Accumulation	Diameter	No. Of	Volume	Accumulation
34	66	9.78	9.78	52	25	3.70	91.26
36	87	12.89	22.67	54	25	3.70	94.96
40	73	10.81	33.48	56	15	2.22	97.19
42	73	10.81	44.30	58	10	1.48	98.67
44	84	12.44	56.74	60	4	0.59	99.26
46	80	11.85	68.59	62	2	0.30	99.56
48	73	10.81	79.41	64	2	0.30	99.85
50	55	8.15	87.56	66	1	0.15	100.00

3.5 Catalytic Activity Testing

Three experiments of hydroisomerization of n-heptane were conducted using HY-zeolite catalysts loaded with different proportions of metals Zr and Pt at a temperature of 275 °C and atmospheric pressure in a gas phase. The products were condensed and analyzed by a GC-FID, as illustrated in Table 4. The weights of the uncondensed light gases (e.g., C₁ + C₂ + C₃) were measured by the differences between the weight of the n-heptane introduced into the reactor with the total weight of the condensed liquid produced from the reaction and then converted into mole fractions. In general, the results of the three experiments of hydroisomerization n-heptane using the three catalysts are plotted in Figure 10-Left, which explains the catalytic performance of the three catalysts. Firstly, the Cat-1 catalyst (2 wt% Zr/HY) performed values of 75.8, 55.7, and 42.2 mol% for conversion, selectivity, and yield, respectively. The conversion of n-heptane was 75.8%, which is considered high due to the elevated catalytic activity of HY-zeolite and its high acidity (i.e., Bronsted type). The second effect comes from adding Zr, which possesses high acidity (i.e., Lewis type). The high conversion showed the strength and activity of the HY-zeolite loaded with Zr metal. Besides, increased cracked and unsaturated components are important in evaluating catalysts. However, it demonstrated low selectivity (55.7 mol%) for isomers due to its high acidity, which may be caused the cracking path to be dominated rather than the isomerization pathway. This resulted in high amounts of low molecular weight cracked products (e.g., C₁-C₃ gases), leading to a low yield of isomers (42.2 mol%). These findings support the conclusions of the other authors [30,39].

The Cat-2 catalyst consisted of 2 wt% Pt/HY and exhibited better catalytic parameters, achieving values of 70.3, 86.0, and 60.4 mol% for conversion, selectivity, and yield, respectively. The effect of Pt metals in enhancing selectivity and yield is much higher than that of Cat-1 catalyst. However, the conversion of n-heptane decreased from 75.8% in Cat-1 to 70.3 mol% in Cat-2. This occurred for two reasons; first, it caused the Pt atoms to occupy the locations of Bronsted acid in the zeolite, leading to a significant decrease in the acidity (i.e., Bronsted type) of the zeolite a reduction in activity. The second reason is that the acidity of Lewis type of Zr is higher than that of Pt metal, which makes the Cat-1 catalyst activity higher than that of the Cat-2 catalyst. In the case of Cat-2, the role of Pt metal in enhancing the selectivity and yield occurred as a consequence of the Pt atoms, which provide a dehydrogenation-hydrogenation function that improved the conversion of long hydrocarbons chains into desired isomers. According to the explanation of the bifunctional mechanism by Mills, Weisz, and Sinfeld [7], these are consistent results with other authors [39-41]. A comparison of n-heptane hydroisomerization products, using the three catalysts shown in Figure 10-Right, illustrates that the produced isomers in Cat-1 were low but increased with Pt metal in Cat-2.

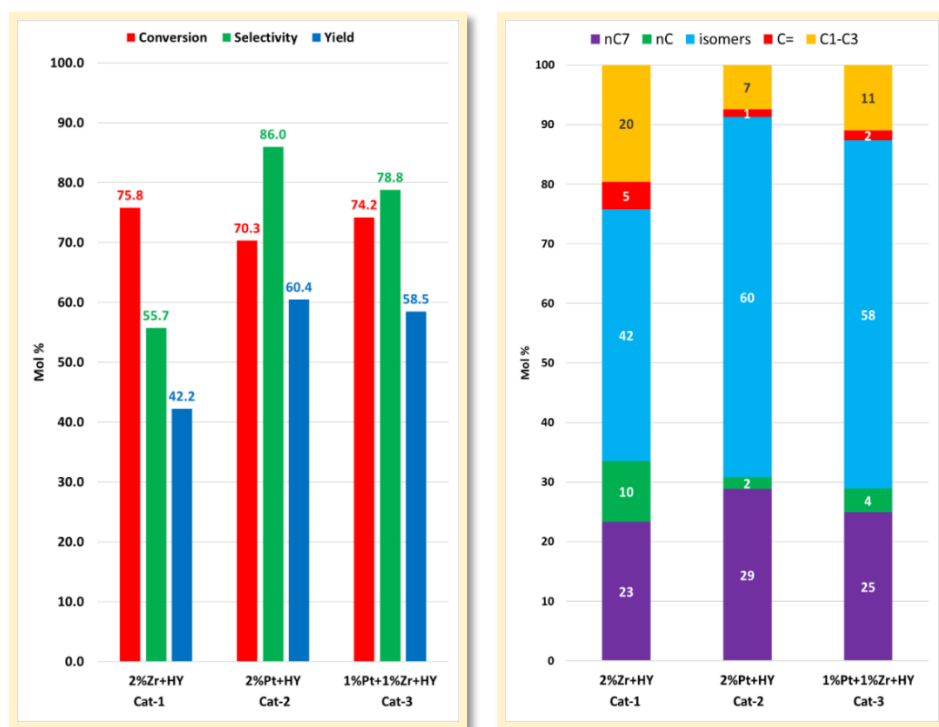


Figure 10: Hydroisomerization of n-heptane, at 275 °C and 1 atm using bimetallic catalysts. (Left): Catalytic activity parameters mol%, (Right) Composition of the products mol%

Table 4: Products composition (mol%) of n-heptane hydroisomerization experiments at 275°C & 1 atm

Component	Cat-1	Cat-2	Cat-3
C1+C2+C3	19.62	7.43	10.96
iC4	3.23	3.63	4.90
nC4	5.11	1.53	2.88
C4=	2.11	0.84	0.88
iC5	2.10	1.28	2.34
nC5	3.85	0.21	0.52
C5=	1.03	0.14	0.29
iC6	0.44	0.23	0.22
nC6	1.29	0.29	0.58
C6=	0.25	0.11	0.12
iC7	36.45	55.30	51.00
nC7	23.30	28.80	24.90
C7=	1.22	0.21	0.41
Total	100.00	100.00	100.00
Σ C=	4.61	1.30	1.70
Σ nC	10.25	2.03	3.98
Σ isomers	42.22	60.44	58.46
Conversion	75.8	70.3	74.2
Selectivity	55.7	86.0	78.8
Yield	42.2	60.4	58.5

At the same time, cracked products, such as C₁-C₃ gases and the not isomerized cracked products, decreased with the use of Pt, resulting in the active role of Pt previously mentioned. In Cat-3 containing 1wt% Zr and 1wt% Pt, the conversion (74.2 mol%) was improved to a level close to that of Cat-1. The selectivity (78.8 mol%) was not significantly decreased from that of Cat-2, leading to a yield (58.5mol%) comparable to that of the costly catalyst containing 2wt%Pt. This enhancement happened due to the concept of bimetallic effect that made the two metals contribute to enhancing the catalytic features of the Pt-Zr/HY catalyst, whereby incorporating Zr metals into zeolites coordination provides an extraordinary Lewis acidity to the zeolite-framework structure. This introduction of Zr metal enhanced the activity and selectivity of the Cat-3 bimetallic catalyst Cat-3. This interpretation of the loaded metal's behavior was further supported by other researchers [22-25,38]. The Cat-3 catalyst simultaneously took advantage of the electronic and catalytic properties of the Zr and Pt metals to enhance its novel catalytic features, reaching a yield of isomers close to that of Cat-2 containing 2 wt% Pt. In other words, it enables the manufacture of a catalyst with half the proportion of the rare and expensive Pt metal in the Cat-2 catalyst, halving the cost of the catalyst.

4. Conclusions

Currently, Pt/zeolites catalysts are a pivotal part of the petroleum refining industry. The escalating prices of Pt metal made catalysts' producers search for ways to decrease the content of Pt metals by using another metal. By studying the promotional effects of Zr on the Pt/HY-zeolite catalysts for n-heptane hydroisomerization, it was found that adding a small ratio of Zr metal can enhance Lewis acidity of Pt/HY-zeolites catalysts (i.e., increase the conversion) without significant impacts on the selectivity to isomers. The benefits of Pt addition are that it increases the selectivity of C₇ isomers and decreases hydrogenolysis/cracking activity that usually produces unwanted C₁-C₃ gases. Furthermore, incorporating Zr increases total acidity, which accounts for the increase in catalytic activity compared with Pt/HY-zeolite. Furthermore, the presence of Zr plays a role in the redistribution of acidic sites with different strengths, enabling to decrease in the content of the very expensive Pt metal, which this cheap Zr metal could partially substitute. This study managed to synthesize an active bimetallic Cat-3 catalyst for hydroisomerization n-heptane that consisted of 1 wt% Pt- and 1 wt% Zr-HY-zeolite, achieving values of 74.2, 78.8, and 58.5 mol% for conversion, selectivity, and yield, respectively. Such achievement gave a good performance comparable to that of the expensive Cat-2 catalyst containing 2 wt% Pt. In addition, it was proven that a small amount of Zr can be used as a partial substitute for the costly Pt noble metal, making the goal of reducing Pt content real, practical, and economical.

Abbreviations and symbols

AFM	Atomic force microscopy
BET	Brunauer, Emmett, and Teller method for surface area measurements
Cat-1	Catalyst composed of 2wt% Pt loaded on HY-Zeolite
Cat-2	Catalyst composed of 2wt% Zr loaded on HY-Zeolite
Cat-3	Catalyst composed of 1wt% Pt and 1wt% Zr loaded on HY-Zeolite
DOC	Degree of Crystallinity
EDX	Energy dispersive X-ray analysis
FWHF	Full width of the peak at half maximum
GC-FID	Gas chromatography- flame ionization detector
HY-zeolite	Acidic form of the zeolite Y type
NaY-zeolite	Sodium form of zeolite Y
NH ₄ -Y-zeolite	Ammonium form of zeolite Y
SEM	Scanning electron microscope
XRD	X-ray diffraction analysis
ZSM-5	ZSM-5 zeolite type
β	β zeolite type

Acknowledgment

The authors would like to express their sincere appreciation to the Department of Chemical Engineering, the University of Technology-Iraq, which helped us complete this work in its laboratories.

Authors contribution

All authors contributed equally to this work.

Funding

This research received no specific grant from any funding agency in the public, commercial, or not-for-profit sectors

Data availability statement

The data that support the findings of this study are available on request from the corresponding author.

Conflicts of interest

The authors declare that there is no conflict of interest.

References

- [1] S. F. Perry, *Isomerization, Industrial & Engineering Chemistry*, ACS Publications, 1948
- [2] Hsu, C. Samuel, and P. R. Robinson. *Petroleum Science and Technology*; Springer, Switzerland, 2019.
- [3] Jones, S. J. David, and P. P. Pujadó, eds. *Handbook of Petroleum Processing*; Springer, Switzerland, 2015.
- [4] Y. Ono, A survey of the mechanism in catalytic isomerization of alkanes. *Catalysis Today* 81 (2003): 3-16. [http://doi:10.1016/S0920-5861\(03\)00097-X](http://doi:10.1016/S0920-5861(03)00097-X).
- [5] P. B. Weisz, Polyfunctional Heterogeneous Catalysis, *Advances in Catalysis*, (1962)137–190. doi: 10.1016/S0360-0564(08)60287-4.
- [6] M. Saito, and T. Iwasaki. Isomerization of Pentanes on Platinum/Rare Earths-Hydrogen-Zeolite Y Catalysts. *Bulletin of The Japan Petroleum Institute* 18 (1976) 117-126. <http://doi.org/10.1627/jpi1959.18.117>

- [7] J. Scherzer, and A. J. Gruia. Hydrocracking science and technology. Crc Press, 1996.
- [8] E. Kikuchi, M. Tsurumi, T. Kimura, and Y. Morita. Isomerization of n-Pentane over Sodium Y Zeolite Exchanged by Palladium and Platinum, Bull. Japan Pet. Inst. 15 (1973) 122-128. <http://doi:10.1627/jpil1959.15.122>.
- [9] T. F. Degnan, Applications of zeolites in petroleum refining. Topics in Catalysis 13 (2000) 349-356. <http://doi:10.1023/A:1009054905137>.
- [10] M. S.-S. Joaquin Pérez Pariente, Structure and Reactivity of Metals in Zeolite Materials. Springer, 2018.
- [11] B. C. Gates, Maria Flytzani-Stephanopoulos, David A. Dixon, and Alexander Katz. Atomically dispersed supported metal catalysts: perspectives and suggestions for future research. Catalysis Science & Technology 7 (2017) 4259-4275. <http://doi.org/10.1039/C7CY00881C>
- [12] J. Liu, Catalysis by supported single metal atoms, Acs Catalysis 7 (2017) 34-59. doi: 10.1021/acscatal.6b01534.
- [13] M. Yang, J. Liu, S. Lee, B. Zugic, J. Huang, L. F. Allard, and M. Flytzani-Stephanopoulos. "A common single-site Pt (II)-O (OH) x-species stabilized by sodium on active and "inert" supports catalyzes the water-gas shift reaction. Journal of the American Chemical Society 137 (2015) 3470-3473. <http://doi:10.1021/ja513292k>.
- [14] L. Guzzi, and I. Kiricsi. Zeolite supported mono-and bimetallic systems: structure and performance as CO hydrogenation catalysts. Applied Catalysis A: General 186 (1999) 375-394. [http://doi.org/10.1016/S0926-860X\(99\)00156-8](http://doi.org/10.1016/S0926-860X(99)00156-8)
- [15] X. Li, and Enrique Iglesia. Pt/[Fe] ZSM-5 modified by Na and Cs cations: an active and selective catalyst for dehydrogenation of n-alkanes to n-alkenes. Chemical communications 5 (2008) 594-596. <http://doi.org/10.1039/B715543C>
- [16] J. Guzman, and Bruce C. Gates. Supported molecular catalysts: metal complexes and clusters on oxides and zeolites. Dalton Transactions 17 (2003) 3303-3318. <http://doi.org/10.1039/B303285J>
- [17] M. Moliner, and A. Corma. Advances in the synthesis of titanosilicates: from the medium pore TS-1 zeolite to highly-accessible ordered materials. Microporous and mesoporous materials 189 (2014) 31-40. <http://doi.org/10.1016/j.micromeso.2013.08.003>
- [18] A. Corma, L. T. Nemeth, M. Renz, and S. Valencia. Sn-zeolite beta as a heterogeneous chemoselective catalyst for Baeyer–Villiger oxidations. Nature 412 (2001): 423-425. <doi.org/10.1038/35086546>
- [19] A. Corma, F. X. Llabres i Xamena, C. Prestipino, M. Renz, and S. Valencia. Water resistant, catalytically active Nb and Ta isolated lewis acid sites, homogeneously distributed by direct synthesis in a beta zeolite. The Journal of Physical Chemistry C 113 (2009): 11306-11315. <http://doi.org/10.1021/jp902375n>
- [20] Y. Zhu, G. Chuah, and S. Jaenicke. Chemo-and regioselective Meerwein–Ponndorf–Verley and Oppenauer reactions catalyzed by Al-free Zr-zeolite beta. Journal of Catalysis 227 (2004): 1-10. <http://doi.org/10.1016/j.jcat.2004.05.037>
- [21] D. J. Lewis, S. V. de Vyver, and Y. Román-Leshkov. Acid–base pairs in Lewis acidic zeolites promote direct aldol reactions by soft enolization. Angewandte Chemie 127 (2015): 9973-9976. <http://doi.org/10.1002/ange.201502939>
- [22] A. Corma, S. Iborra, and A. Velty. Chemical routes for the transformation of biomass into chemicals. Chemical reviews 107(2007): 2411-2502. <http://doi:10.1021/cr050989d>.
- [23] Y. Román-Leshkov, and M. E. Davis. Activation of carbonyl-containing molecules with solid Lewis acids in aqueous media. Acs Catalysis 1 (2011): 1566-1580. <http://doi:10.1021/cs200411d>.
- [24] M. Moliner, State of the art of Lewis acid-containing zeolites: lessons from fine chemistry to new biomass transformation processes. Dalton transactions 43 (2014): 4197-4208. <http://doi.org/10.1039/C3DT52293H>
- [25] Y. H. Luo, J. D. Lewis, and Y. Román-Leshkov. Lewis acid zeolites for biomass conversion: Perspectives and challenges on reactivity, synthesis, and stability. Annual review of chemical and biomolecular engineering 7 (2016): 663-692. <http://doi.org/10.1146/annurev-chembioeng-080615-034551>
- [26] G. X. Yan, A. Wang, I. E. Wachs, and J. Baltrusaitis. Critical review on the active site structure of sulfated zirconia catalysts and prospects in fuel production. Applied Catalysis A: General 572 (2019): 210-225. <http://doi:10.1016/j.apcata.2018.12.012>.
- [27] H. Li, J. Wang, D. Zhou, D. Tian, C. Shi, U. Mueller, M. Feyen et al. Structural stability and Lewis acidity of tetravalent Ti, Sn, or Zr-linked interlayer-expanded zeolite COE-4: A DFT study. Microporous and Mesoporous Materials 218 (2015): 160-166. <http://doi:10.1016/j.micromeso.2015.07.020>.
- [28] W. Jian, W. Zhang, Y. Suo, and Y. Wang. Synthesis of Ni/H-Zr-MCM-48 and their isomerization activity of n-heptane." Journal of Porous Materials 25(2018): 1317-1324. <http://doi:10.1007/s10934-017-0542-7>.
- [29] A. S. Karakoulia, E. Heracleous, and A. A. Lappas. Mild hydroisomerization of heavy naphtha on mono-and bi-metallic Pt and Ni catalysts supported on Beta zeolite. Catalysis Today 355 (2020): 746-756. <http://doi:10.1016/j.cattod.2019.04.072>.

- [30] L. E. Kitaev, Z. M. Bukina, V. V. Yushchenko, N. S. Nesterenko, and L. N. Alekseenko. Acidic and catalytic properties of dealuminated zeolite Y treated with zirconyl nitrate solution. *Petroleum Chemistry* 46 (2006): 246-256. <http://doi:10.1134/S0965544106040049>.
- [31] L. Yang, Z. Song, Y. Yu, L. Zhu, and D. Xia. Bimetallic Bifunctional Pt-NiP/H β as a Novel and Highly Efficient Catalyst for n-Hexane Isomerization. *Catalysis Surveys from Asia* 24 (2020): 104-114. <http://doi:10.1007/s10563-020-09295-4>.
- [32] B. Y. S. Al-Zaidi, The effect of modification techniques on the performance of zeolite-Y catalysts in hydrocarbon cracking reactions, Ph.D. Thesis, The University of Manchester, (United Kingdom), 2011.
- [33] H. Robson, *Verified synthesis of zeolitic materials*. Gulf Professional Publishing, 2001.
- [34] S. Colin Cundy and P. A. Cox. The hydrothermal synthesis of zeolites: Precursors, intermediates and reaction mechanism. *Microporous and mesoporous materials* 82 (2005): 1-78. <http://doi:10.1016/j.micromeso.2005.02.016>.
- [35] W. Arthur Chester and E. G. Derouane. *Zeolite characterization and catalysis*. 360. New York, EUA: Springer, 2009.
- [36] A. Sayari, *Recent advances and new horizons in zeolite science and technology*. Studies in Surface Science and Catalysis, 1996.
- [37] V. Meynen, P. Cool, and E. F. Vansant. *Verified syntheses of mesoporous materials*. *Microporous and mesoporous materials*, 125 (2009) 170-223. <https://doi.org/10.1016/j.micromeso.2009.03.046>
- [38] H. Ma, J. Zhang, M. Wang, and S. Sun. Modification of Y-Zeolite with Zirconium for Enhancing the Active Component Loading: Preparation and Sulfate Adsorption Performance of ZrO (OH) 2/Y-Zeolite. *ChemistrySelect*. 4 (2019) 7981-7990. <http://doi:10.1002/slct.201901519>.
- [39] M. J. Ramos, J. P. Gomez, F. Dorado, P. Sánchez, and J. L. Valverde. Hydroisomerization of a refinery naphtha stream over platinum zeolite-based catalysts. *Chem. Eng. J.* 126 (2007): 13-21. <http://doi:10.1016/j.cej.2006.08.026>.
- [40] Z. B. Wang, A. Kamo, T. Yoneda, T. Komatsu, and T. Yashima. Isomerization of n-heptane over Pt-loaded zeolite β catalysts. *Applied Catalysis A: General* 159 (1997): 119-132. [http://doi:10.1016/S0926-860X\(97\)00059-8](http://doi:10.1016/S0926-860X(97)00059-8)
- [41] L. Ping, Y. A. O. Yue, X. Zhang, and W. A. N. G. Jun. Rare earth metals ion-exchanged β -zeolites as supports of platinum catalysts for hydroisomerization of n-heptane. *Chinese Journal of Chemical Engineering* 19 (2011): 278-284. [http://doi:10.1016/S1004-9541\(11\)60166-3](http://doi:10.1016/S1004-9541(11)60166-3).